Jurnal Polimesin
Department of Mechanical Engineering
State Polytechnic of Lhokseumawe
http://e-jurnal.pnl.ac.id/polimesin

e-ISSN : 2549-1999 No. : 2 Month : April
p-ISSN : 1693-5462 Volume : 24 Year : 2026

Processing dates: received on 2026-1-07, reviewed on 2026-02-19, accepted on 2026-03-14 and online availability on 2026-04-25

# The effect of heat input on defect formation, macrostructure, microstructure and hardness in AA 1100 aluminum weld joints using the GMAW process

**Rizki Dwi Ardika[1*], Ilham Sulthoni[1], Munaji[1], Yoyok Winardi[1], Muizuddin Azka[2]**
[1]Department of Mechanical Engineering, Muhammadiyah University of Ponorogo, Ponorogo, 63471, Indonesia
[2]Research Center for Process and Manufacturing Industry Technology, National Research and Innovation Agency (BRIN), Tangerang Selatan, 15314, Indonesia
*Corresponding author: rizkidwiardika@umpo.ac.id

## Abstract
AA 1100 aluminum is widely used in industrial applications due to its low density and good corrosion resistance; however, welding defects such as porosity and changes in mechanical properties often occur during Gas Metal Arc Welding (GMAW). One of the most influential parameters on weld quality is the welding current. This study analyzes the effect of welding current variations on the physical and mechanical properties of AA 1100 GMAW welded joints using ER 5356 filler wire. Welding was carried out at currents of 100 A, 130 A, and 160 A using argon shielding gas. The welded joints were evaluated by visual inspection, macrostructure observation, microstructure analysis, and Vickers microhardness testing. The test results showed that increasing the welding current resulted in wider weld beads, increased porosity and spatter defects, as well as coarser grain structures in the heat-affected zone (HAZ) and weld metal. The lowest porosity and spatter occurred at 100 A, while the highest porosity and spatter occurred at 160 A. This was due to excessive heat input and hydrogen trapping. Microstructural analysis revealed the presence of $FeAl_3$ intermetallic phases dispersed within the aluminum matrix. The highest hardness value was found in the weld metal region at 100 A, which was caused by the finer grain size and the strengthening effect of Mg from the ER 5356 filler. Overall, this study confirmed that the welding current significantly affects the defect formation, microstructural evolution, and hardness distribution of GMAW AA 1100 weld joints.

**Keywords:**
Aluminum alloy, welding defects, porosity, current, Gas Metal Arc Welding (GMAW)

## 1 Introduction
As times become more advanced, metal materials are increasingly used in a wide range of applications. One of these is aluminum (Al). Aluminum is widely used due to its several advantages, including its light weight, high strength, and good corrosion resistance [1]. This material is widely applied in aircraft parts, shipyards, trains, and automotive vehicle bodies because it is lighter than steel [2]. However, aluminum alloys have several disadvantages. Among them are high specific heat and conductivity, ease of oxidation, and the formation of $Al_2O_3$, which has a high melting point. In addition, aluminum alloys solidify quickly, leading to the formation of fine hydrogen cavities [3].

In joining aluminum (Al) metal, Gas Metal Arc Welding (GMAW) is often used [4]. GMAW welding uses shielding gases, such in argon (Ar) and carbon dioxide ($CO_2$), to prevent the weld metal from being contaminated by the surrounding air. GMAW welding has several advantages, including high speed and work efficiency, as well as the ability to weld large quantities at a fast rate due to the use of a continuous wire electrode that supplies material continuously. However, GMAW also has limitations, one of which is its susceptibility to hydrogen diffusion, which can trigger porosity defects [5]. Porosity is one of the most common defects found in aluminum welding. This defect is caused by hydrogen from water vapor in the air, so humidity is an important parameter that must be controlled. During the welding process, hydrogen can be trapped in the weld metal and form gas bubbles, which ultimately result in pores in the weld joint [6]. In addition, the GMAW welding process has limitations, including being unsuitable for certain types of materials, such as thin metals or metals with reflective properties. One way to overcome porosity is to properly regulate the flow.

The selection of current parameters needs to be considered, because the current can cause structural changes due to the cooling process that can affect the materials's strength. Therefore, the current setting in the welding process plays an important role in the quality of the welding results [7]. Fundamentally, the welding current is the primary factor that determines the heat input in the Gas Metal Arc Welding (GMAW) process as it controls the thermal energy delivered to the material per unit length of the weld. Heat input is influenced by the current, voltage and welding speed, thus directly affecting the stability of the weld pool, penetration depth, cooling rate, microstructural evolution and defect formation [8]. An improper current setting during welding process can cause porosity in the weld metal [9]. When the current is too low, the heat generated is insufficient to completely melt the metal, so the gas formed in the weld pool is trapped and forms small cavities. Conversely, too high a current can cause the weld pool to become too fluid and unstable, so that the shielding gas cannot properly protect the welding area, and outside air can enter the molten metal. This condition results in the formation of pores in the weld which can reduce the strength and quality of the joint. Therefore, selecting the correct current is crucial to ensure the welding process runs optimally and produces a joint with good physical and mechanical properties.

Based on previous studies, investigations into GMAW-welded joints of AA 1100 aluminum using varying currents to reduce porosity remain limited. Most previous studies focused on steel materials and evaluated only tensile properties without comprehensively analyzing defect-formation mechanisms. This study fills this gap by focusing on AA 1100 welded using GMAW and analyzing the effect of welding current as an indicator of heat input on the characteristics of the welded joint. Therefore, this study aims to investigate the effect of welding current on porosity formation, microstructural evolution, and hardness distribution in AA 1100 GMAW welded joints**.** This study establishes a correlation between current variation, porosity formation, microstructural evolution, and hardness distribution in the base metal, heat-affected zone (HAZ) and weld metal. Thus, this study provides a more comprehensive understanding of the defect mechanisms and the relationship between microstructure and hardness in AA 1100 welds, which is still limited.

## 2 Research methods
### 2.1 Material preparation and welding process
AA 1100 aluminum alloy plates with dimensions of 150mm×150mm×6mm were welded using ER 5356 filler wire (SOWESCO-Pinnacle Alloys, Houston, TX, USA) with a diameter of 1.0 mm. The chemical compositions of both materials are presented in Table 1. The welding process was performed using GMAW (Gas Metal Arc Welding) with GEKAMAC 420 (Gedik Welding, Turkey) using 99% argon shielding gas at a controlled flow rate of 15 L/min under direct current electrode positive (DCEP) polarity. The welding technique applied was forehand (forward) from right to left, as shown in Fig. 1. The welding parameters varied were currents of 100, 130, and 160 A, while the arc voltage was

maintained at 22 V and the travel speed was kept constant at 30 cm/min (5 mm/s). Based on these parameters, the calculated heat inputs were 0.3520 kJ/mm (100 A), 0.4576 kJ/mm (130 A), and 0.5632 kJ/mm (160 A). The welding specimen (coupon test) used a butt joint configuration as shown in Fig. 2, and the geometry design of the V-shaped groove is presented in Fig. 3.

Table 1. The chemical composition of AA 1100 and ER 5356 (wt%)

| Material | Si | Fe | Cu | Mn | Mg | Zn | Cr | Ti | Al |
|---|---|---|---|---|---|---|---|---|---|
| AA1100 | 0.95 | 0.95 | 0.15 | 0.05 | - | 0.10 | - | - | 99 |
| ER5356 | 0.25 | 0.40 | | 0.12 | 4.5 | 0.10 | 0.15 | 0.10 | bal |

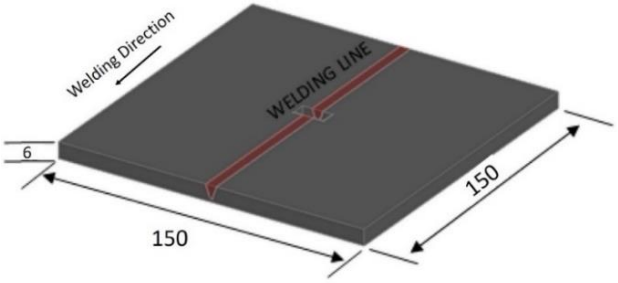


**Fig. 1.** Welding technique forehand (mm)

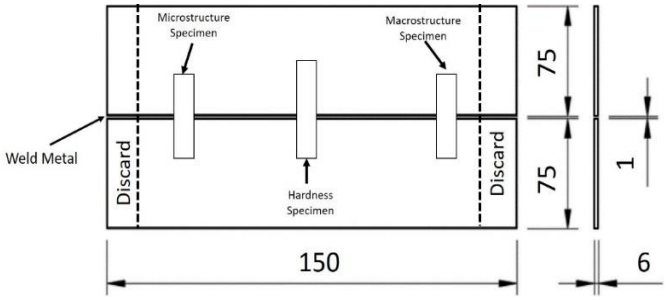


**Fig. 2.** Coupon test (mm)

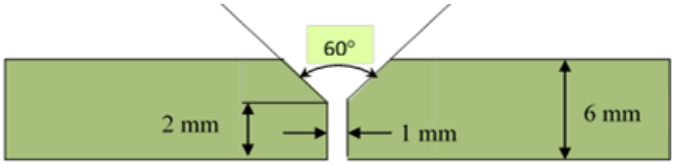


**Fig. 3.** Geometry of the welding specimen

### 2.2 Welded joint characterization

Weld-bead observation aims to observe and identify defects on the surface of welded specimens. Weld bead observation was performed using a Redmi 10 camera (Beijing, China) at 1.0x magnification.

Macrostructure observation was performed using an Olympus SZ 1145 TR stereomicroscope (Tokyo, Japan) at 1.5x magnification. Microstructure observation was performed using a Euromex microscope (Arnhem, The Netherlands) at 100x magnification. The standard procedure for microstructure observation includes cutting, polishing with 200-5000 grit sandpaper, and finally etching. Etching was performed according to ASTM E407-07 with a Poulton reagent solution consisting of 30 mL HCl, 40 mL $HNO_3$, 2.5 mL HF, 42.5 mL $H_2O$, and 12 g $CrO_3$. The observed areas included the base metal, heat-affected zone (HAZ), and weld metal.

Hardness testing was performed using a Vickers Highwood testing machine type HWMMT-X7 (Fukushima, Japan). The indenter used was a diamond pyramid with a load of 200 gf and a pressure of 10 seconds in accordance with ASTM E384. The hardness areas tested were the base metal, HAZ, and weld metal. The indentations were made along the cross-section of the weld joint at a depth of approximately 0.5 mm below the polished surface to minimize the influence of surface preparation effects.

## 3 Result and discussion

### 3.1 Bead defects observation

Visual observations conducted on the weld joint revealed various weld-bead shapes. Weld-bead observations were carried out on the bottom and top surfaces of the welded specimen. This was done to see the characteristics of the weld bead under 3 different currentconditions, as shown in Fig. 4.

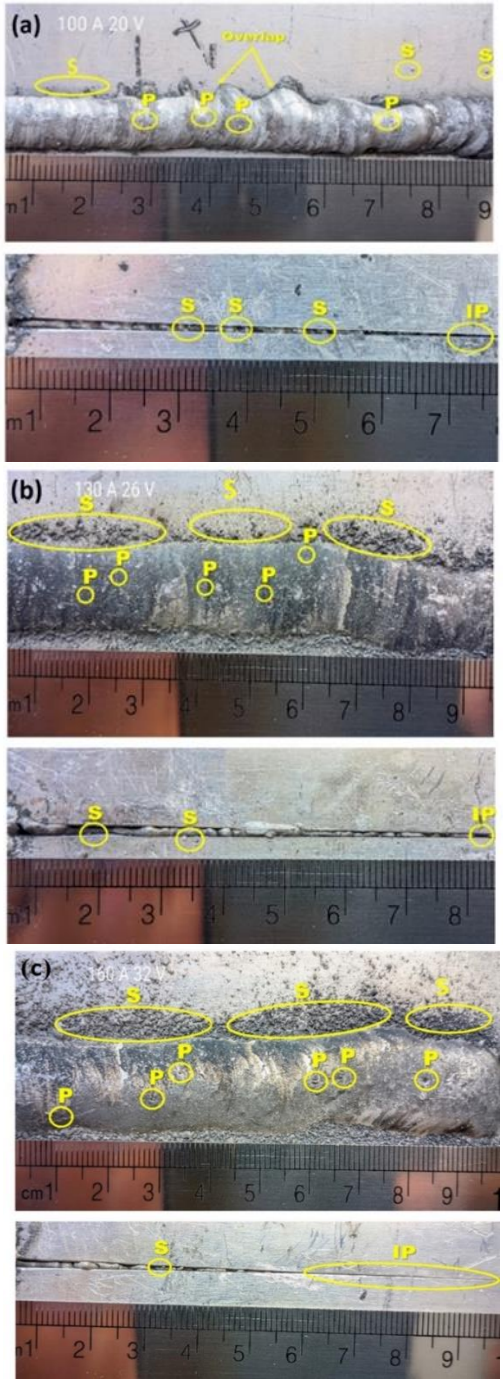


**Fig. 4.** Appearance of weld beads from welding: (a) 100 A, (b) 130 A, (c) 160 A.

Based on the observation results, the weld bead at the 100 A current welding joint appears relatively small and stacked. Meanwhile, at the 130 A current variation, the weld bead is formed more evenly and slightly wider. Meanwhile, the 160 A current produces a wider weld bead than the other two variations. This shows that the higher the current, the greater the effect will be on the width of the weld bead. The wider weld bead is caused by the higher welding current, which will result in increased temperature and heat input, resulting in a wider weld bead. In addition, a high welding current can increase the heat energy in the welding arc, melting the

base metal over a wider area, resulting in a larger weld pool and spreading to the sides.

Welding defects identified in AA 1100 joints include porosity (P), spatter (S), incomplete penetration (IP), and overlap (O). The number of each defect is shown in Table 2. Identification was carried out by visual inspection of the entire surface of the weld bead, which has a length of approximately 150 mm and a bead width of approximately 150 mm, resulting in a visual inspection area of approximately 300 mm² for each specimen. This method only detects defects on the outer surface and does not cover internal defects in the weld metal. The least porosity defects were found in the 100 A weld joint. The amount of porosity in the 130 A weld joint increased, and the 160 A weld joint had the highest amount of porosity. This indicates that the higher the welding current, the greater the amount of porosity. The increased porosity is caused by the high current, resulting in increased heat input. Increased heat input affects the increase in temperature around the weld pool. High temperatures cause the weld pool to become very large, dilute, and turbulent, so that hydrogen gas is easily trapped in the molten metal. Hydrogen that is trapped and cannot escape from the weld pool due to rapid cooling and does not have enough time to diffuse out before solidification causes the formation of porosity in the weld joint. This is in accordance with Kramer research [10] which states that the higher the hydrogen content, the greater the porosity. In contrast, at a current of 100 A the weld pool is smaller and more stable, allowing for more effective hydrogen gas release and resulting in less porosity.

Spatter is a welding defect characterized by the escape of molten metal from the weld pool [11]. Based on observations in this study, spatter occurred at all welding current variations, but the amount varied across conditions. The highest spatter was found at a current of 160 A, while the lowest was at 100 A. These results indicate that increasing the welding current tends to be followed by an increase in spatter at the weld joint [12]. This condition is related to differences in heat input and arc stability during the GMAW process. At a current of 100 A, the heat energy generated by the arc is relatively lower, resulting in a more stable transfer of molten metal from the electrode tip to the weld pool with a moderate melting rate. Molten metal droplets can enter the weld pool in a more controlled manner without breaking up, resulting in relatively little spatter. Conversely, at a current of 160 A, the heat input and arc energy increase significantly, resulting in a faster electrode melting rate and increased arc pressure. This condition causes molten metal to be more easily ejected from the weld pool due to increased weld pool turbulence and arc instability. Even though an inert argon shielding gas is used, spatter can still occur because the primary function of the shielding gas is to protect the weld pool from atmospheric contamination, not to control the metal transfer mechanism. Therefore, spatter formation in the GMAW process is more strongly influenced by welding parameters such as current, heat input, and arc stability, which determine the characteristics of metal droplet transfer from the electrode to the weld pool.

Incomplete penetration is another defect that appears on the bottom surface of the weld joint and occurs in weld joints of all current types. The 100 A weld joint has the highest number of incomplete penetration defects compared to the 130 A and 160 A weld joints. This is because the heat input generated at 100 A is not good enough to melt the base metal to the root of the weld joint perfectly. A low welding current results in less heat energy released by the welding arc, and causes the weld pool to become shallower. Thus, the molten metal does not reach the root of the joint and does not achieve deep penetration in the weld joint. Lu stated that incomplete penetration can cause a decrease in the strength of the weld joint [11]. The last welding defect to appear is an overlap. Overlap occurs only in the 100 A weld joint and does not occur at 130 A or 160 A. The low welding current results in insufficient arc heat to melt the base metal at the edge of the joint, so the molten weld metal does not have enough time to fuse with the parent metal, resulting in a wider, protruding weld lip.

Table 2. Defects identified by visual observations.

| No | Variation | Defects | Amount |
|---|---|---|---|
| 1 | 100 A | Porosity (P) | 4 |
| | | Spatter (S) | 13 |
| | | Incomplete Penetration (IP) | 4 |
| | | Overlap (O) | 2 |
| 2 | 130 A | Porosity (P) | 5 |
| | | Spatter (S) | 28 |
| | | Incomplete Penetration (IP) | 2 |
| 3 | 160 A | Porosity (P) | 8 |
| | | Spatter (S) | 47 |
| | | Incomplete Penetration (IP) | 1 |

### 3.2 Macrostructure

Welded joints were subjected to macrostructural observations focusing on the amount of porosity in all types of welded joints. The results of macrostructural observations revealed that 160 A welded joints had the most porosity defects, as seen in Fig. 5. Welded joints with 100 A tended to have small amounts of porosity, with a current of 130 A, the size decreased and increased. At a current of 160 A, the porosity decreased, but the amount increased. High currents increase the temperature in the welding area, accelerating hydrogen diffusion into the weld pool. Hydrogen atoms that combine and settle in the weld metal will become porosity [1].

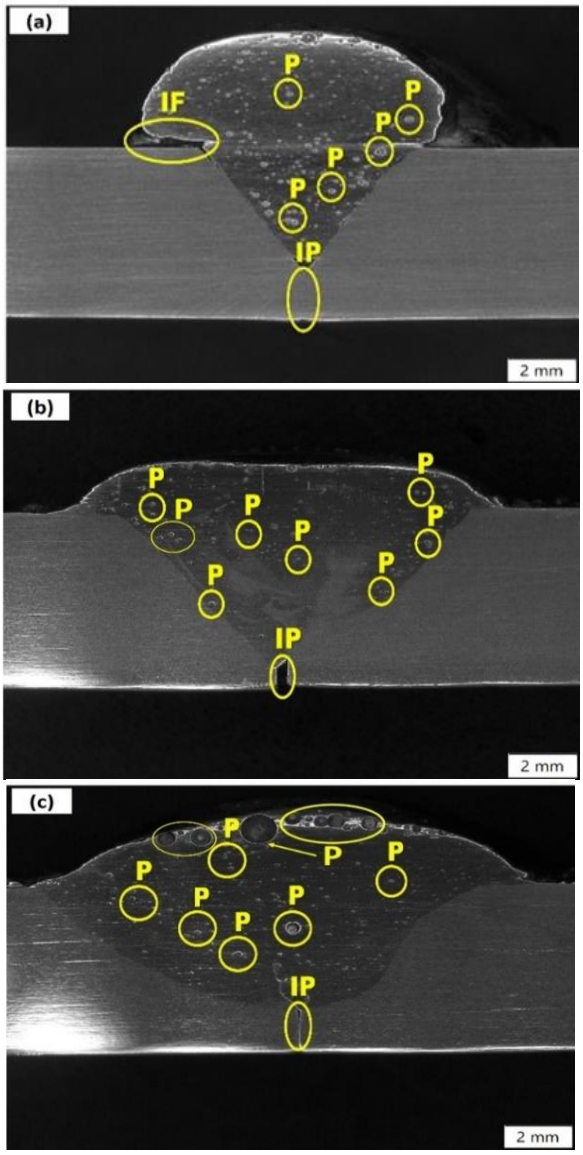


**Fig.5.** Macrostructure of welded joints at (a) 100 A, (b) 130 A, (c) 160 A.

The mechanism of porosity formation in welded joints is shown in Fig. 6. Gas in the form of hydrogen will dissolve into the weld metal during welding. Hydrogen will easily dissolve in weld metal when it is in a liquid state and at high temperatures. The solubility level decreases as the freezing process progresses from the liquid weld metal phase change to semi-solid and then to solid [12]. Aluminum, which initially contains hydrogen in the liquid state, then rejects hydrogen during the freezing process. This causes the presence of gas bubbles in the weld metal [13]. The bubbles that form cannot escape because the aluminum is semi-solid and is trapped between growing crystals [14]. This mechanism shows that hydrogen bubbles will move upwards, become trapped and settle on the surface. The presence of bubbles that settle and cannot escape in the weld metal area causes the formation of porosity in the weld metal area [15]. Porosity defects in welds can disrupt the structural integrity and mechanical properties of welded joints. Porosity can be minimized by proper current regulation and good environmental management.

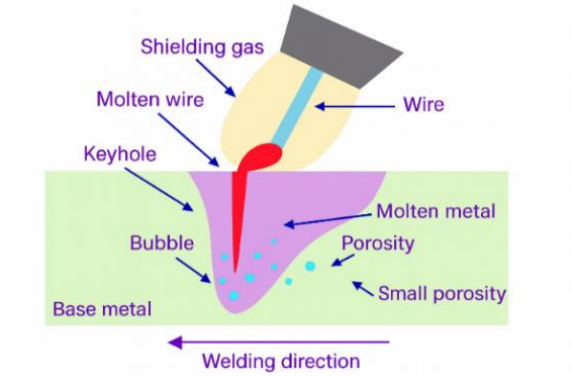


**Fig. 6.** Mechanism of porosity formation in welding

### 3.3 Microstructure

Microstructure testing is used to determine the phase changes and grain size of the weld metal, HAZ, and base metal, as shown in Fig. 7. Changes in the microstructure phase and grain size cause changes in the mechanical properties of aluminum.

The results of microstructure testing in the base metal area of the welded joint using currents of 100 A, 130 A, and 160 A show no changes in the microstructure of both grains and grain boundaries. This is because in the base metal area, there is no heating process during the welding process, and the heat received is relatively small. There is no significant difference in grain shape to the microstructure of the three currents used. In the microstructure test above, there is a $FeAl_3$ phase; this phase is a mixture of iron (Fe) and aluminum (Al). In the figure, the black particles evenly dispersed in the aluminum matrix are $Al_3Fe$ [16].

The formation of the HAZ microstructure in 1100 aluminum is limited to recovery, recrystallization, and grain growth. Welding results in annealing in the HAZ, increasing in grain size [17]. The HAZ microstructure in weld joints with currents of 130 A and 160 A appears coarser. This may be because the observed grain size changes are a result of the influence of the welding current applied during the welding process. Grain size changes in the HAZ depend on temperature, heating duration, material characteristics, and cooling rate [18]. Meanwhile, at a current variation of 100 A, the grain shape appears smoother. This is due to the lower heat influence compared to other variations. The image above shows that cooling around the HAZ is slower, resulting in a coarser grain structure in the HAZ.

In the weld metal area, the weld joint produced at 100 A shows fine, relatively uniform grains. Lower welding current reduces heat input and decreases the thermal energy around the weld metal. According to previous research conducted by Zhu et al., (2017) [19], changes in heat input during welding can affect the thermal cycle of the joint and influence the width of the HAZ and the grain-formation process. Welded joints at low temperature conditions will produce a weld metal structure with uniform, fine and distributed grains. Meanwhile, at 130 A, the grain size increases, and at 160 A, the grains appear coarser. This is because the weld metal area experiences an increase in heat input, resulting in slower cooling, and coarser grains. Coarse grains will cause a decrease in the strength of the welded joint [20]. This is supported by research conducted by Qi et al., (2024), who found that high heat input during welding causes the microstructure in the HAZ to expand, so that the microstructure becomes coarse [21].

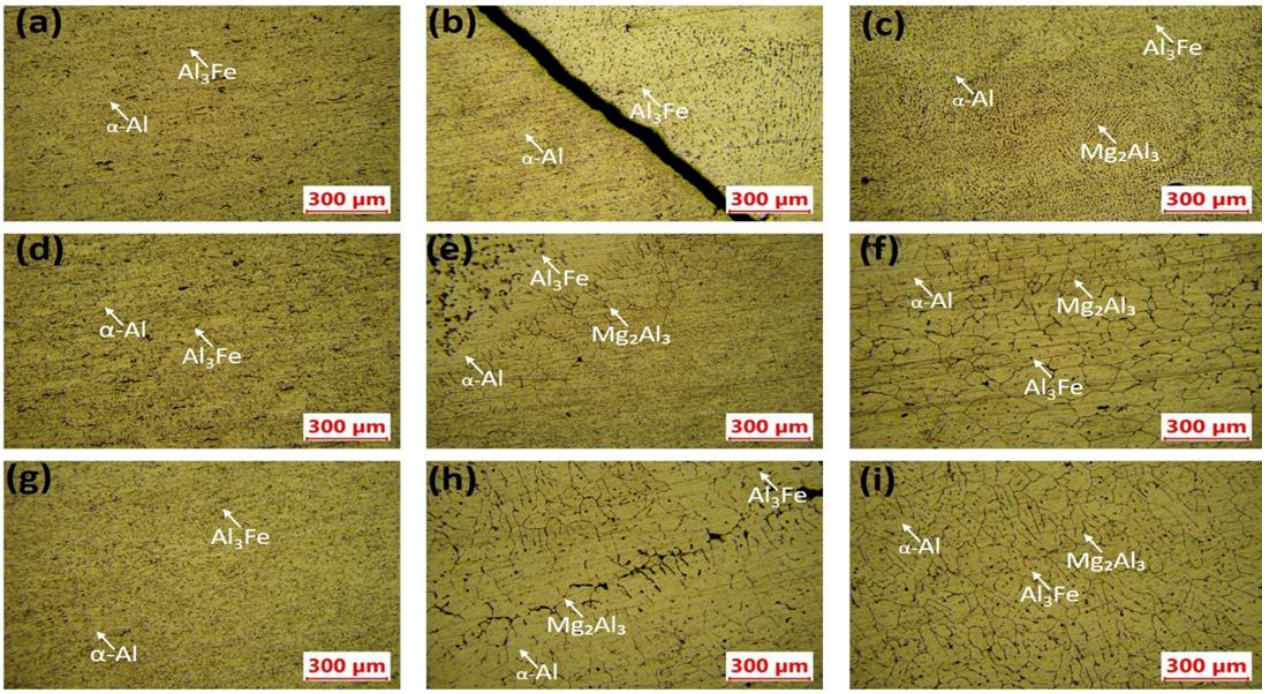


**Fig. 7.** Microstructure of base metal area: (a) 100 A, (d) 130 A, (g) 160 A; Microstructure of the HAZ area: (b) 100 A, (e) 130 A, (h) 160 A; Microstructure of weld metal area: (c) 100 A, (f) 130 A, (i) 160 A.

### 3.4 Vickers microhardness

Hardness testing was conducted to evaluate the hardness distribution in the base metal (BM), heat-affected zone (HAZ), and weld metal (WM) regions, as shown in Fig. 8. The highest hardness value in the BM region was obtained at a welding current of 100 A, at 74.03 HVN, while the lowest hardness value, at 66.76 HVN, was obtained at a weld joint with a current of 130 A. In the HAZ region, the highest hardness value was also found at 100 A, 72.01 HVN, while the lowest was at 160 A, 62.73 HVN. Meanwhile, in the WM region, the highest hardness value was obtained at 100 A, 89.97 HVN, while the lowest was at 160 A, 81.92 HVN.

The relatively high hardness value found in the weld metal is influenced by the use of ER5356 filler metal. AA1100 is considered commercially pure aluminum, while ER5356 electrode wire contains alloying elements, particularly magnesium (Mg). The presence of Mg in the filler metal contributes to increased strength and hardness through a solid-solution strengthening mechanism [22]. Furthermore, the welding current also plays a significant role in determining the thermal conditions during the welding process. Increasing the current leads to increased heat input, which results in a slower cooling rate and encourages grain growth in the weld joint area. High heat input can also increase the likelihood of porosity defects in the weld metal, ultimately reducing the mechanical properties of the joint and reducing its ductility [23] [24]. These results align with the research by Senthilkumar et al. (2023), which showed that heat input significantly influences the microstructure and mechanical properties of welded joints [25].

In the HAZ, hardness values are generally lower than those of the base metal because this area undergoes thermal cycling during the welding process without melting. This heat exposure triggers recovery, recrystallization, and grain growth in the aluminum matrix. This process causes a decrease in dislocation density and an increase in grain size. According to the Hall–Petch relationship, increasing grain size reduces resistance to dislocation movement, thereby decreasing the material's hardness. Furthermore, increasing the welding current increases the heat input, slowing the cooling rate and accelerating the grain growth process in the HAZ. This phenomenon explains the observed decrease in hardness in the HAZ at higher welding currents.

Overall, the hardness distribution in a welded joint is influenced by a combination of factors, namely the filler metal composition, heat input during welding, grain size evolution, and the presence of welding defects such as porosity. Therefore, controlling welding parameters, particularly the welding current, is crucial for maintaining a finer microstructure and achieving better hardness characteristics in AA1100 GMAW welded joints.

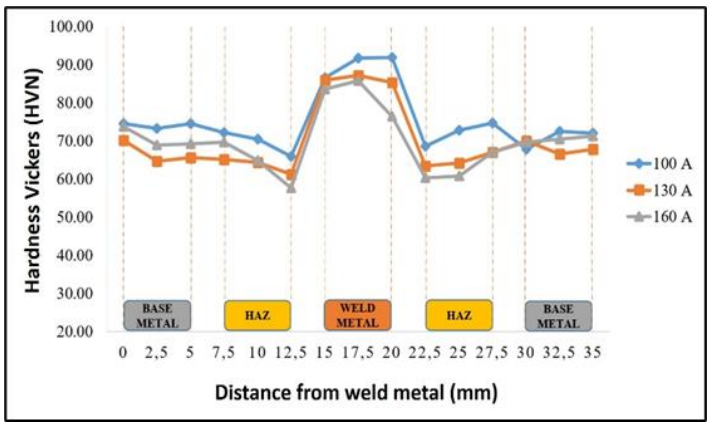


**Fig. 8.** Hardness test results for the proposed specimen

## 4 Conclusion

This study analyzed the effect of welding current on the physical and mechanical properties of AA 1100 weld joints. The following conclusions can be drawn:

1. Variations in welding current significantly affect the quality of AA 1100 GMAW weld joints, particularly in terms of weld defects, microstructure, and hardness.
2. Higher welding currents increase heat input, leading to increased porosity and spatter defects and wider weld beads, with the highest number of defects occurring at 160 A (0.5632 kJ/mm**)**.
3. A lower welding current of 100 A (0.3520 kJ/mm) produces minimal porosity, a finer weld metal microstructure, and the highest hardness.
4. Higher heat input at higher welding currents promotes coarser grain growth, thereby decreasing weld joint hardness. Therefore, proper current control is essential to achieve optimal physical and mechanical properties.
5. Based on the combined evaluation of weld defects, microstructure, and hardness distribution, a welding current of 100 A (heat input 0.3520 kJ/mm) is recommended as the optimal parameter for GMAW welding of AA 1100.


## Acknowledgment

The authors would like to thank the Muhammadiyah University of Ponorogo and National Research and Innovation Agency (BRIN), for the collaborative research.


## References


[1] M. Dada and P. Popoola, "Recent advances in joining technologies of aluminum alloys: a review," *Discov. Mater.*, vol. 4, no. 1, p. 86, 2024. doi: 10.1007/s43939-024-00155-w

[2] C. Zhang, M. Gao, and X. Zeng, "Journal of Materials Processing Technology Effect of microstructural characteristics on high cycle fatigue properties of laser-arc hybrid welded AA6082 aluminum alloy," *J. Mater. Process. Tech.*, vol. 231, pp. 479–487, 2016, doi: 10.1016/j.jmatprotec.2016.01.019.

[3] Y. Han, S. Xue, R. Fu, L. Lin, Z. Lin, Y. Pei, and H. Sun, "Influence of hydrogen embrittlement on impact property and microstructural characteristics in aluminum alloy weld," *Vacuum*, vol. 172, no. November 2019, pp. 1–8, 2020, doi: 10.1016/j.vacuum.2019.109073.

[4] D. Y. Kim, I. Hwang, G. Jeong, M. Kang, D. Kim, J. Seo, and Y. M. Kim, "Effect of porosity on the fatigue behavior of gas metal arc welding lap fillet joint in GA 590 MPa steel sheets," *Metals (Basel).*, vol. 8, no. 4, 2018, doi: 10.3390/met8040241.

[5] M. Chludzinski, L. Garcia-Sesma, O. Zubiri, N. Rodriguez, and E. Aldanondo, "Investigation of the Effects of Gas Metal Arc Welding and Friction Stir Welding Hybrid Process on AA6082-T6 and AA5083-H111 Aluminum Alloys," *Metals (Basel).*, vol. 15, no. 9, p. 1005, 2025.

[6] M. Orlando, M. De Maddis, V. Razza, and V. Lunetto, "Non-destructive detection and analysis of weld defects in dissimilar pulsed GMAW and FSW joints of aluminium castings and plates through 3D X-ray computed tomography," *Int. J. Adv. Manuf. Technol.*, vol. 132, no. 5, pp. 2957–2970, 2024, doi: 10.1007/s00170-024-13576-x.

[7] D. Zhao, M. Ivanov, Y. Wang, and W. Du, "Welding quality evaluation of resistance spot welding based on a hybrid approach," *J. Intell. Manuf.*, vol. 32, no. 7, pp. 1819–1832, 2021.

[8] C. Chen, G. Sun, W. Du, Y. Li, C. Fan, and H. Zhang, "Influence of heat input on the appearance, microstructure and microhardness of pulsed gas metal arc welded Al alloy

weldment," *J. Mater. Res. Technol.*, vol. 21, pp. 121–130, 2022, doi: 10.1016/j.jmrt.2022.09.028.
[9] J. C. Garcia-guerrero, F. F. Curiel-López, V. H. López-Morelos, J. J. Taha-Tijerina, T. J. Sánchez-Cruz, M. C. Ramirez-Lopez, E. Cortes-Carillo, and M. A. Quinones-Salinas, "Impact of Welding Parameters in the Porosity of a Dissimilar Welded Lap Joint of CP800-XPF1000 Steel Weldment by GMAW-P," Metals., vol. 14 no. 3, p. 139, 2024, doi: 10.3390/met14030309
[10] S. Kramer, V. Lubkowitz, M. Haas, J. Michel, C. Spurk, A. Olowinsky, G. A. Faria, M. Jarwitz, T. Graf, V. Schulze, and F. Zanger, "Investigation of the formation and reduction of hydrogen porosity during laser welding of additively manufactured AlSi10Mg parts," Int J Adv Manuf Technol., vol 142, pp. 6105–6123, 2026. doi: 10.1007/s00170-025-17198-9.
[11] K. Lu, J. Lin, Z. Chen, W. Wang, and H. Yang, "Safety assessment of incomplete penetration defects at the root of girth welds in pipelines," *Ocean Eng.*, vol. 230. December 2020, p. 109003, 2021, doi: 10.1016/j.oceaneng.2021.109003.
[12] N. Cui, T. Zhao, Z. Wang, Y. Zhao, Y. Chao, H. Lin, D. Li, and J. Zhao, "Porosity evolution mechanisms, influencing factors, and ultrasonic-assisted regulation in joining high Mg-content aluminum alloys," *J. Mater. Process. Tech.*, vol. 336, no. October 2024, p. 118706, 2025, doi: 10.1016/j.jmatprotec.2024.118706.
[13] A. M. Samuel, E. Samuel, and V. Songmene, "A Review on Porosity Formation in Aluminum-Based Alloys," 2023.
[14] N. Béraud, A. Chergui, M. Limousin, F. Villeneuve, and F. Vignat, "An indicator of porosity through simulation of melt pool volume in aluminum wire arc additive manufacturing," vol. 1, pp. 1–8, 2022.
[15] S. Huang, L. Xu, M. Lou, H. Chen, K. Zhang, and Y. Li, "Keyhole-induced pore formation mechanism in laser-MIG hybrid welding of aluminum alloy based on experiment and multiphase numerical model," *J. Mater. Process. Tech.*, vol. 314, no. August 2022, p. 117903, 2023, doi: 10.1016/j.jmatprotec.2023.117903.
[16] K. J. Pranav, S. P. Sibi, and P. P. Jana, "Evolution of Fe-rich intermetallic phases in cast and wrought aluminium alloys: Microstructural insights and property correlations," *J. Alloys Compd.*, vol. 1042, no. September, p. 184101, 2025, doi: 10.1016/j.jallcom.2025.184101.
[17] A. V. Jebaraj, K. V. V. Aditya, T. S. Kumar, L. Ajaykumar, and C. R. Deepak, "Mechanical and corrosion behaviour of aluminum alloy 5083 and its weldment for marine applications," *Mater. Today Proc.*, vol. 22, pp. 1470–1478, 2019, doi: 10.1016/j.matpr.2020.01.505.
[18] H. Deng, Z. Liu, X. Wang, J. Ma, F. Han, and Z. Wang, "Effect of heat input on the microstructure and mechanical properties of the simulated coarse-grained heat-affected zone (CGHAZ) of novel twining-induced plasticity (TWIP) steel," *Mater. Today Commun.*, vol. 33, p. 104407, 2022.
[19] C. Zhu, X. Tang, Y. He, F. Lu, and H. Cui, "Effect of preheating on the defects and microstructure in NG-GMA welding of 5083 Al-alloy," *J. Mater. Process. Technol.*, vol. 251, no. May 2017, pp. 214–224, 2018, doi: 10.1016/j.jmatprotec.2017.08.037.
[20] K. G. Vorkachev, P. P. Stepanov, L. I. Éfron, M. M. Kantor, A. V Chastukhin, and S. V Zharkov, "Effect of microstructure on high-strength low-alloy steel welded joint toughness with simulation of heat-affected zone coarse-grained area," *Metallurgist*, vol. 64, no. 9, pp. 875–884, 2021.
[21] H. Qi, Q. Pang, W. Li, and S. Bian, "Effect of high welding heat input on the microstructure and low-temperature toughness of heat affected zone in magnesium-treated EH36 steel," *Sci. Rep.*, vol. 14, no. 1, p. 19459, 2024.
[22] A. V. Jebaraj, K. V. V Aditya, T. S. Kumar, L. Ajaykumar, and C. R. Deepak, "ScienceDirect Mechanical and corrosion behaviour of aluminum alloy 5083 and its weldment for marine applications," *Mater. Today Proc.*, vol. 22, pp. 1470–1478, 2020, doi: 10.1016/j.matpr.2020.01.505.
[23] R. D. Ardika, T. Triyono, N. Muhayat, and Triyono, "A review porosity in aluminum welding," *Procedia Struct. Integr.*, vol. 33, no. C, pp. 171–180, 2021, doi: 10.1016/j.prostr.2021.10.021.
[24] N. Muhayat, R. D. Ardika, A. M. Kadir, E. P. Budiana, and T. Triyono, "Simultaneous Enhancement of Welder Health and Aluminum Weld Joint Quality Using Controlled Welding Room Condition," 2024.
[25] S. Senthilkumar, S. Manivannan, R. Venkatesh, and M. Karthikeyan, "Influence of heat input on the mechanical characteristics, corrosion and microstructure of ASTM A36 steel welded by GTAW technique," *Heliyon*, vol. 9, no. 9, 2023.